

1
2 **Responses of globally important phytoplankton species to olivine dissolution products and**
3 **implications for carbon dioxide removal via ocean alkalinity enhancement**
4
5
6
7
8
9
10
11

12 David A. Hutchins^{1†*}, Fei-Xue Fu¹, Shun-Chung Yang¹, Seth G. John¹, Stephen J. Romaniello²,
13 M. Grace Andrews², Nathan G. Walworth^{1,2,3†*}
14
15
16
17
18
19
20
21
22
23
24
25
26
27
28

29 ¹University of Southern California, Los Angeles, CA, USA

30 ²Vesta, PBC, San Francisco, CA, USA

31 ³J. Craig Venter Institute, La Jolla, CA, USA

32
33 †These authors contributed equally to this work

34 *Correspondence: David A. Hutchins - dahutch@usc.edu, Nathan G. Walworth –
35 nate@vesta.earth
36

37
38
39
40
41
42
43
44
45
46
47
48
49
50
51
52
53
54
55
56
57
58
59
60
61
62
63
64
65
66
67
68

Abstract

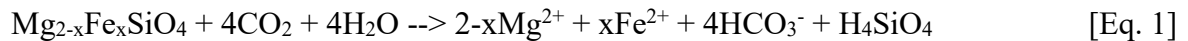
Anthropogenic greenhouse gas emissions are leading to global temperature increases, ocean acidification, and significant ecosystem impacts. Given current emissions trajectories, the IPCC reports indicate that rapid abatement of CO₂ emissions and development of carbon dioxide removal (CDR) strategies are needed to address legacy and difficult to abate emissions sources. These CDR methods must efficiently and safely sequester gigatons of atmospheric CO₂. Coastal Enhanced Weathering (CEW) via the addition of the common mineral olivine to coastal waters is one promising approach to enhance ocean alkalinity for large-scale CDR. As olivine weathers, it releases several biologically active dissolution products, including alkalinity, trace metals, and the nutrient silicate. Released trace metals can serve as micronutrients but may also be toxic at high concentrations to marine biota including phytoplankton that lie at the base of marine food webs. We grew six species representing several globally important phytoplankton species under elevated concentrations of olivine dissolution products via a synthetic olivine leachate (OL) based on olivine elemental composition. We monitored their physiological and biogeochemical responses, which allowed us to determine physiological impacts and thresholds at elevated olivine leachate concentrations, in addition to individual effects of specific constituents. We found both positive and neutral responses but no evident toxic effects for two silicifying diatoms, a calcifying coccolithophore, and three cyanobacteria. In both single and competitive co-cultures, silicifiers and calcifiers benefited from olivine dissolution products like iron and silicate or enhanced alkalinity, respectively. The non-N₂-fixing picocyanobacterium could use synthetic olivine-derived iron for growth, while N₂-fixing cyanobacteria could not. However, other trace metals like nickel and cobalt supported cyanobacterial growth across both groups. Growth benefits to phytoplankton groups *in situ* will depend on species-specific responses and ambient concentrations of other required nutrients. Results suggest olivine dissolution products appear unlikely to cause negative physiological effects for any of the phytoplankton examined, even at high concentrations, and may support growth of particular taxa under some conditions. Future studies can shed light on long-term eco-evolutionary responses to olivine exposure and on the potential effects that marine microbes may in turn have on olivine dissolution rates and regional biogeochemistry.

69 Introduction

70

71 Excess anthropogenic greenhouse gas emissions are driving global changes to Earth
72 systems and leading to simultaneous increases in sea surface temperatures, ocean acidification,
73 and regional shifts in nutrient supplies (IPCC, 2022). To counteract these trends and limit the
74 average global temperature increase to 1.5-2°C, carbon dioxide removal (CDR) methods that can
75 collectively remove and permanently store gigatons of atmospheric CO₂ (GtCO₂) must be
76 developed (Rogelj et al., 2018). Coastal Enhanced Weathering (CEW) with olivine (Mg₂-
77 _xFe_xSiO₄) has been proposed as an economically scalable form of ocean alkalinity enhancement
78 (OAE), as it is a globally abundant, naturally occurring ultramafic silicate mineral (Taylor et al.,
79 2016; Caserini et al., 2022). Olivine is considered to be one of the most favorable minerals for
80 CDR as it weathers quickly under Earth surface conditions (Oelkers et al., 2018). Like other
81 silicate minerals, it dissolves in water to release cations (Mg²⁺, Fe²⁺) and generates alkalinity
82 (principally HCO₃⁻), with up to 4 mol of CO₂ sequestered per mol of olivine [Eq. 1].
83

84



85

86 Forsteritic olivine is the magnesium-rich end-member of olivine and can contain various other
87 trace constituents. For example, olivine used in this study contains ~92% magnesium (Mg²⁺) and
88 ~8% ferrous iron (Fe²⁺) along with trace amounts (<1%) of other metals such as nickel (Ni),
89 chromium (Cr), and cobalt (Co). As olivine weathers, it releases several biologically important
90 dissolution products into the surrounding seawater: (I) bicarbonate (HCO₃⁻) and carbonate ion
91 (CO₃²⁻), hereafter summarized as “alkalinity”; (II) silicic acid (Si(OH)₄) hereafter termed
92 silicate; (III) and a variety of trace metals including iron (Fe²⁺, or oxidized aqueous species),
93 nickel (Ni²⁺), cobalt (Co²⁺), and chromium (CrVI). These dissolution products have the potential
94 to affect important phytoplankton functional groups like silicifying algae (diatoms), calcifying
95 algae (coccolithophores), and cyanobacteria, which lie at the base of marine food webs and drive
96 the biological carbon pump (Hauck et al., 2016; Moran, 2015). Hence, it is important to
97 understand the specific effects of these constituents on globally important phytoplankton species,
98 particularly at elevated concentrations to simulate large-scale CEW applications.

99

100 Significant alkalinity additions from olivine weathering can consume CO₂ from the
101 surrounding seawater, causing a CO₂ deficit until air-sea equilibration. This shift in the carbonate
102 system from CO₂ to HCO₃⁻/CO₃²⁻ by transient, non-equilibrated OAE may affect phytoplankton
103 functional groups differently, with some taxa being more sensitive than others. For example, it is
104 predicted that calcifying organisms like coccolithophores may benefit from CEW due to
105 decreases in proton concentrations (H⁺) and increases in the CaCO₃ saturation state.
106 Additionally, dissolving one mole of olivine leads to a one mole increase in dissolved silicate,
107 which is an essential and often bio-limiting nutrient for silicifying organisms like diatoms, a
108 phytoplankton group estimated to contribute up to 40% of the marine primary production
(Bertrand et al., 2012). Hence, diatoms may especially benefit from CEW applications with

109 olivine. Additionally, diatoms are particularly noted for being dominant phytoplankton in the
110 coastal regimes where olivine deployments are likely to take place (Field et al., 1998). While
111 there are both planktonic and benthic species of diatoms, the latter will presumably be exposed to
112 especially sustained and elevated levels of dissolution products when olivine is deployed in
113 natural marine sediments. It is unknown if either group, calcifiers or silicifiers, may consistently
114 outcompete the other following CEW with olivine (Bach et al., 2019).

115 Trace metals like Fe and Ni are general micronutrients required by all classes of
116 phytoplankton and could potentially support their growth upon fluxes into seawater from olivine
117 weathering. In particular, dinitrogen (N₂)-fixing cyanobacteria and diatoms both have elevated
118 Fe requirements (Hutchins and Sañudo-Wilhelmy, 2021; Hutchins and Boyd, 2016), and so may
119 stand to benefit from increases in Fe concentrations. Although a required micronutrient at low
120 levels, in high enough concentrations Ni may potentially negatively impact phytoplankton
121 growth, although one recent study showed limited to no toxic effects of very high Ni
122 concentrations (e.g. 50,000 nmol L⁻¹) for several phytoplankton taxa (Guo et al., 2022). Cobalt
123 can also serve as a micronutrient for phytoplankton (Sunda and Huntsman, 1995; Hawco et al.,
124 2020) but may also be toxic at high concentrations (Karthikeyan et al., 2019). However, other
125 trace metals found with olivine such as Cr are not nutrient elements and also need to be
126 considered in terms of their possible toxicity to phytoplankton (Flipkens et al., 2021; Frey et al.,
127 1983).

128 Hence, it is important to understand the taxon-specific effects of these constituents to
129 determine thresholds at which key phytoplankton functional groups may experience positive or
130 negative effects. Furthermore, it is important to expose phytoplankton to elevated concentrations
131 of olivine dissolution products simultaneously to understand what impacts may occur for large
132 CEW applications. Exposures of organisms to concentrated olivine dissolution products also
133 provides an “worst case scenario” benchmark, which can be compared to lower actual
134 environmental exposures resulting from small CEW additions, slower olivine dissolution time
135 scales, and dilution from advection. While olivine weathers relatively quickly compared to other
136 silicate minerals (Hartmann et al., 2013), dissolution of olivine grains is gradual (i.e. years)
137 relative to microbial physiological responses (hours), posing a challenge to test different
138 concentrations of olivine constituents on phytoplankton physiology. To address this, we prepared
139 a synthetic olivine leachate (OL) composed of olivine dissolution products with trace metal
140 concentrations well over those of seawater (7-12,000 times higher), in order to represent a “worst
141 case” scenario for a CEW project. This extreme scenario was estimated based on the maximum
142 expected impact of olivine weathering on the chemistry of the overlying water column.
143 Assuming a 10 cm thick layer of pure olivine sand dissolves with a 100 year half-life into 1
144 meter of overlying water with a 24 hour residence time, the anticipated steady state change in the
145 alkalinity of the overlying water column is 65 umol/kg (assuming 4 moles of alkalinity per mole
146 olivine (Meysman and Montserrat, 2017) and 100% release to the water column). The
147 concentrations of other components were chosen assuming stoichiometric, congruent dissolution
148 and quantitative release to the water column as well -- a worst case scenario. Furthermore,

149 phytoplankton were exposed to OL within a small, enclosed batch culture. We cultured 6 species
150 representing three globally important phytoplankton functional groups: 2 diatoms (*Nitzschia*,
151 *Ditylum*), 1 coccolithophore (*Emiliana*), 2 dinitrogen (N₂) fixing cyanobacteria (*Trichodesmium*,
152 *Crocospaera*), and 1 non-N₂ fixing picocyanobacterium (*Synechococcus*). All of these species
153 are planktonic, with the exception of the diatom *Nitzschia* which frequently forms benthic
154 biofilms (Yamamoto et al., 2008). Cultures were grown semi-continuously in natural seawater
155 based modified Aquil media (Sunda et al., 2005) with OL as the only available Fe source (and Si
156 source for diatoms). For all experiments, cultures were sampled for a basic set of core
157 biogeochemical and physiological parameters (Fu et al., 2005, 2008; Tovar-Sanchez et al., 2003;
158 Paasche et al., 1996). This approach allowed us to compare phytoplankton taxon-specific
159 responses, including: **1**) physiological impacts at extremely high OL concentrations, **2**)
160 physiological thresholds and dose responses across a range of increasing concentrations of OL,
161 and **3**) individual effects of specific OL constituents.

162

163 **Materials and Methods**

164

165 *Culture growth conditions and experimental set up*

166

167 Six species of phytoplankton were used in these experiments, including: the planktonic diatom
168 *Ditylum brightwellii* (centric, planktonic, isolated by T. Ryneerson from Narragansett Bay,
169 Rhode Island, USA) and the benthic diatom *Nitzschia punctata* (CCMP 561, isolated from tidal
170 mud near San Diego, North Pacific Ocean), a coccolithophore, *Emiliana huxleyi* (CCMP 371, a
171 North Atlantic isolate), a picoplanktonic cyanobacterium *Synechococcus sp.* (strain XM-24,
172 isolated by J. Zheng from Xiamen estuary, the South China Sea, PRC, belonging to clade CB5,
173 subcluster 5.2), and two marine dinitrogen (N₂) fixing cyanobacteria, *Trichodesmium erythraeum*
174 (strain IMS 101, from the Gulf Stream, Northwest Atlantic Ocean) and *Crocospaera watsonii*
175 (WH 0005, from the North Pacific Ocean). Cultures were grown in 500 mL polycarbonate flasks
176 at 28°C for the three cyanobacteria, and 20°C for the diatoms and *Emiliana huxleyi*. Cool-white
177 fluorescent light was supplied following a 12:12 light:dark cycle at an irradiance level of 150
178 $\mu\text{Em}^{-2}\text{s}^{-1}$. Stock cultures were grown in natural offshore seawater collected with trace metal clean
179 methods (John et al., 2022), which was used to make modified Aquil Control Medium (ACM).
180 The positive control ACM contained replete levels of nutrients and trace metals (i.e., 4 μM
181 phosphate (PO_4^{3-}), 60 μM nitrate (NO_3^-), 250 nM Fe, 50 nM Co, no Cr or Ni, (Sunda et al.,
182 2005)), and 60 μM silicate (SiO_3^{2-}) was added to the ACM medium for culturing the two diatoms
183 only.

184 For experiments, cultures were inoculated into the three Olivine Leachate (OL) treatments
185 described below, with the addition of 4 μM phosphate (PO_4^{3-}) and 60 μM nitrate (NO_3^-). There
186 was no nitrogen (N) added into the ACM or OL medium for the N₂ fixers. Iron, Cobalt, Nickel
187 (Fe, Co and Ni) and silicate (SiOH_4) were not added to the OL medium, except as components of
188 the olivine leachate (see below). The background nutrient concentrations in the collected natural

189 seawater were $1\mu\text{M NO}_3^-$, $0.1\mu\text{M PO}_4^{3-}$ and $3\mu\text{M SiOH}_4$. Dissolved trace metals were not
 190 measured, but surface concentrations are typically very low (1nM Fe or less, (John et al., 2012))
 191 at the SPOT time series site where the seawater was cleanly collected, relative to amounts added
 192 to the ACM and to the OL (**Table 1**) for phytoplankton culturing.

193
 194 *Synthetic olivine leachate preparation*

195
 196 To simulate acute exposure of phytoplankton to elevated levels of olivine dissolution products in
 197 seawater, we prepared an artificial concentrated OL stock solution based on elemental analyses
 198 of commercial ground olivine rock (Sibelco. (2022) Technical Data - Olivine Refractory Grade
 199 Fine. Antwerp, Belgium). For experimental exposures, this concentrated OL stock was added to
 200 seawater growth medium to yield the final concentrations shown in **Table 1**, which will be
 201 referred to throughout as a “100%” concentration of OL. Experiments examining biological
 202 effects across a dilution range (0-100%) used correspondingly lower additions of the
 203 concentrated stock.

204
 205 **Table 1.** Concentrations of added ions or compounds in serial dilutions of synthetic olivine
 206 leachate (OL, 0% to 100%) used in the phytoplankton growth experiments; and concentrations of
 207 components in the three concentrated stocks used to prepare experimental medium (1mL/L
 208 added for 100% OL). Stock C was prepared in 10 nM HCl to keep the trace metals in solution
 209 until addition.

	OL Added	Mg ²⁺ (μM)	SiOH ₄ (μM)	OH ⁻ (μM)	Fe(II) (μM)	Ni(II) (μM)	Cr(VI) (μM)	Co(II) (μM)
Concentration added to growth medium	100%	44.9	25	100	3.36	0.13	0.12	0.006
	80%	35.9	20	80	2.7	0.10	0.10	0.005
	50%	22.5	12.3	50	1.7	0.07	0.06	0.003
	30%	13.5	7.5	30	1.0	0.04	0.04	0.002
	10%	4.5	2.5	10	0.34	0.01	0.01	0.001
	0%	0	0	0	0	0	0	0
Concentrated stock solutions (mM)		MgCl ₂	NaSiO ₂	NaOH	FeCl ₂	NiCl ₂	K ₂ CrO ₄	CoCl ₂
Stock A		44.9						
Stock B			25	100				
Stock C					3.36	0.13	0.12	0.006

210
 211 *Experimental methods*

212
 213 Semi-continuous culturing methods were used to achieve nearly steady-state growth. Cultures
 214 were diluted with fresh medium every 2 or 3 days, using in vivo fluorescence as a real time
 215 biomass indicator. Dilutions were calculated to bring the cultures back down to the biomass

216 levels that were recorded after the previous day's dilution. In this way, cultures were allowed to
217 determine their own growth rates under each set of experimental conditions, without ever nearing
218 stationary phase, significantly depleting nutrients or self-shading (Fu et al., 2022). For all
219 experiments, cultures were sampled for a basic set of core biomass and physiological parameters,
220 including cell counts, CO₂ fixation, particulate organic carbon (POC), particulate organic
221 nitrogen (PON), particulate organic phosphorus (POP) and biogenic silica (BSi, diatoms only)
222 once steady-state growth was obtained for each growth condition (typically after 8–10
223 generations). Steady-state growth status was defined as no significant difference in cell- or in
224 vivo-specific growth rates for at least 3 consecutive transfers.

225

226 There were four sets of experiments in this project:

227

228 *1) Acute responses to elevated olivine leachate levels.* The goal of this set of experiments was to
229 investigate the responses of the diatoms *Nitzschia* and *Ditylum* to relatively high concentrations
230 of olivine leachate, in order to determine acute exposure responses. To see if the leachate may
231 have a positive or negative effect on their physiology, they were compared to their respective
232 control cultures. There were a total of three treatments consisting of: OL (100%), ACM, and
233 ACM with low Fe/Si (with 2 nM Fe EDTA added, and no added SiOH₄).

234

235 *2) Responses to a broad range of olivine leachate levels.* In these experiments, *Synechococcus*,
236 *Crocospaera*, *Ditylum*, and *Emiliania huxleyi* were grown in culture medium across a series of
237 OL dilutions (Table 1) to determine their responses across a range of leachate concentrations,
238 from high to very low-level exposures.

239

240 *3) Fe bioavailability and Cr toxicity from olivine leachate to N₂-fixing cyanobacteria.* The goal
241 of this set of experiments was to investigate OL-derived Fe bioavailability to N₂-fixing
242 cyanobacteria, *Trichodesmium* and *Crocospaera*. An additional experiment was conducted to
243 investigate potential Cr(VI) toxicity.

244

245 *4) Two species co-culture competition experiments during olivine leachate exposure.* In order to
246 test how OL may affect co-existence and competition between the diatom *Ditylum* and the
247 coccolithophore *Emiliania huxleyi*, a simple batch co-culture competition experiment was carried
248 out in which the 2 species were inoculated at a 1:1 ratio (based on equivalent levels of cellular
249 Chlorophyll a due to the large differences in their cell sizes) into 100% OL and regular ACM,
250 and grown for 10 days until early stationary phase. In vivo fluorescence and cell counts were
251 monitored daily. Relative abundance and growth rates of the two species were determined based
252 on microscopic cell counts during the exponential growth phase of the mixed cultures. Biogenic
253 silica (BSi, an indicator of diatom abundance) and particulate inorganic carbon (PIC or calcite,
254 an indicator of coccolithophore abundance) were collected every other day in order to further
255 determine how these two species responded to co-culture with and without leachate additions.

256
257
258
259
260
261
262
263
264
265
266
267
268
269
270
271
272
273
274
275
276
277
278
279
280
281
282
283
284
285
286
287
288
289
290
291

Analytical methods

Determination of growth rates and chlorophyll a Growth rates were determined based on changes in chlorophyll a. For chlorophyll a determination, subsamples of 30 ml from each triplicate bottle were GF/F filtered, extracted in 6 ml of 90% acetone, stored overnight in the dark at -20°C , and chlorophyll a concentrations were measured fluorometrically using a Turner 10-AU fluorometer (Welschmeyer, 1994). Specific growth rates were determined using the equation:

$$\mu = \frac{\ln\left(\frac{N_{T_{final}}}{N_{T_{initial}}}\right)}{T_{final} - T_{initial}}$$

where μ is the specific growth rate (per day) and N is the chlorophyll a concentration at $T_{initial}$ and T_{final} (Kling et al., 2021).

Particulate C, N, P and Si. Particulate organic carbon and nitrogen (CHN) samples from all experiments were filtered (pre-combusted GF/F) and frozen for analysis using a Costech Elemental Analyzer (Hutchins et al., 2007). Samples for biogenic silica (BSi) were filtered onto 25 mm diameter, 0.6 μm pore size polycarbonate filters (Pall Life Sciences), and analyzed according to (Brzezinski, 1985). POP (particulate organic phosphorus) samples were collected onto pre-combusted 25 mm GF/F filters and analyzed as in Fu et al. 2005 (Fu et al., 2005).

Primary productivity. For all species other than the coccolithophore (see below), primary production was measured in triplicate using 24h incubations (approximating net PP) with H^{14}CO_3 under the appropriate experimental growth conditions for each treatment (Fu et al., 2008). CO_2 fixation rates were calculated using measured final experimental DIC concentrations and biomass. All samples for primary production were counted using a Wallac System 1400 liquid scintillation counter.

Photosynthetic and calcification rates of *Emiliana huxleyi*. For the coccolithophore, two 40 mL subsamples from each triplicate bottle were spiked with 0.5 μCi $\text{NaH}^{14}\text{CO}_3$. One subsample was incubated in the light and the other in the dark for 24 h. Then two sets of 20 mL aliquots from each sub-sample were filtered onto Whatman GF/F filters. The filters for photosynthetic rate determination were fumed with saturated HCl before adding scintillation cocktail fluid. Photosynthetic rate and calcification rate were calculated as described in Paasche et al. 1996 (Paasche et al., 1996).

292 Nitrogen fixation rates of *Crocospaera watsonii*. In order to estimate the N₂ fixation rates of
293 *Crocospaera*, initial and final particulate organic nitrogen samples (50mL) were collected on
294 combusted GF/F filters over a 24 hr incubation. The PON specific N₂ rates were calculated using
295 the following equation:

$$Nfix = \frac{\left(\frac{PON_{T_{final}} - PON_{T_{initial}}}{PON_{T_{initial}}} \right)}{T_{final} - T_{initial}}$$

296
297
298
299 where Nfix is the N specific N₂ fixation rates (day⁻¹) and PON is the particulate organic nitrogen
300 at T_{initial} and T_{final} as measured using an elemental analyzer (Costech Analytical
301 Technologies) (Fu et al., 2014)
302

303 Fe quota. Intracellular Fe content was determined by filtering culture samples onto acid-washed
304 0.2-µm polycarbonate filters (Millipore), and rinsing with oxalate reagent to remove extracellular
305 trace metals (Tovar-Sanchez et al., 2003). Fe was determined with a magnetic sector-field high-
306 resolution inductively coupled plasma mass spectrometer (ICPMS) (Element 2, Thermo) (Jiang
307 et al., 2018; John et al., 2022).
308

309 Statistical methods. A one-way ANOVA analysis of variance was used to analyze differences
310 between treatments using Prism 8. Differences between treatments were considered significant at
311 p<0.05. Post-hoc comparisons were conducted using the Tukey's multiple comparison test to
312 determine any pairwise differences. Equality of variance was verified for all data using F tests,
313 and the Shapiro Wilk test was used to test for significant departures from normality, which was
314 not the case for any of our data sets. For experiments with only one or two OL treatments and
315 the ACM control, graphs are presented with each treatment marked with a letter denoting
316 significant differences at the p < 0.05 level from each of the other treatments. For experiments
317 such as OL dilution series with many treatments (7 in this case), clear visualization of differences
318 with all other treatments using letters is not feasible. For these experiments, significant
319 differences in the OL treatments relative to the ACM positive control are indicated by asterisks
320 (* = p < 0.05; ** = p < 0.01; *** = p < 0.001; **** = p < 0.0001). For all experiments, actual p
321 values are given in the text.
322
323

324 **Results**

326 *Diatoms*

327 We hypothesized that the diatoms might benefit from the OL products Si and Fe, as they
328 are both required for growth and can be limiting for this group (Tréguer et al., 2018). Hence, we
329 grew the benthic diatom *Nitzschia* across three treatments: 100% OL alone, Aquil control
330 medium (ACM), and ACM but with low, limiting Si and Fe concentrations (ACM-low-SF).
331 *Nitzschia* grew and fixed carbon just as well in the 100% OL as the ACM (p=0.35; p=0.21),

332 while showing reduced rates in the ACM-low-SF treatment ($p=0.02$; $p < 0.0001$; **Fig. 1A, B**).
 333 Likewise, the particulate Si:C ratios demonstrated 100% OL to be just as good a source of Si to
 334 *Nitzschia* as the ACM ($p=0.98$), and considerably better than the ACM-low-SF ($p=0.0012$; **Fig.**

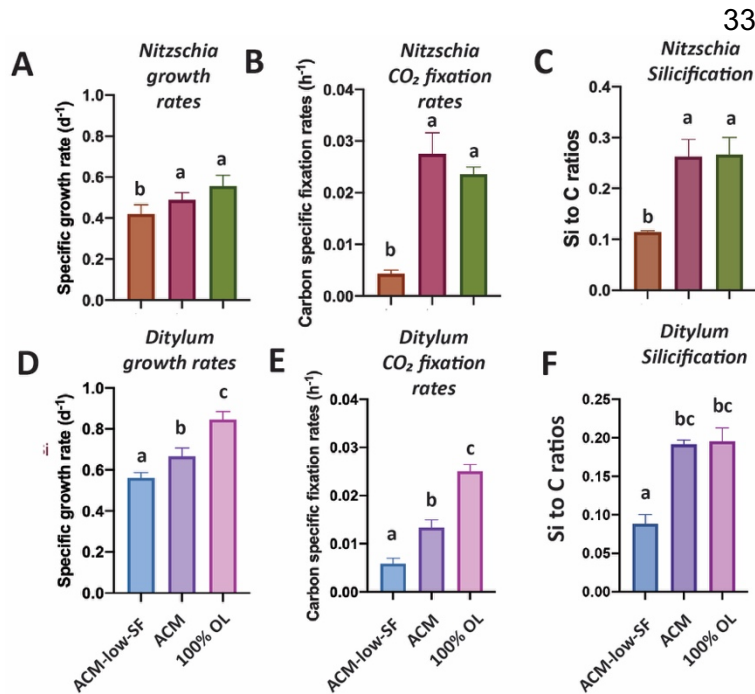


Fig 1. Effects of olivine leachate versus culture medium controls on growth and physiology of a benthic and pelagic diatom. A) and D) are Cell-specific growth rates (d⁻¹), B) and E) are Carbon-specific fixation rates (hr⁻¹) and C) and F) are Si:C ratios (mol:mol) for the diatoms *Nitzschia punctata* (benthic) and *Ditylum brightwellii* (pelagic), respectively. Abbreviations: OL is 100% olivine leachate, ACM is positive control Aquil medium, ACM-low-SF is positive control Aquil medium with lowered Si and Fe concentrations. Y-axis values represent the means, and error bars are the standard deviations of biological triplicate cultures for each treatment. Different letters indicate significant differences at the $p < 0.05$ level.

Growth and CO₂ fixation rates of the planktonic diatom *Ditylum* were significantly higher in the 100% OL treatment compared to either the ACM ($p=0.002$; $p=0.0001$) or ACM-low-Si/Fe treatments ($p=0.0002$; $p < 0.0001$; **Fig. 1D, E**), while Si:C ratios were the same ($p=0.93$; **Fig. 1F**). When *Ditylum* was grown across a range of OL concentrations (i.e., a dilution series from 0% to 100% additions, where 100% corresponds to the 100% OL treatment), we observed increasing growth and CO₂ fixation rates with increasing OL concentrations, with maximum rates observed at and above 50% of the original OL that were not significantly different from those in the ACM control ($p=0.06$, 0.33, 0.99, **Fig. 2A, B**). *Ditylum* particulate Si:C ratios also reached levels not significantly different to those seen in the

363 ACM medium in the 100% additions ($p=0.07$, **Fig. 2C**). Likewise, *Ditylum* cellular Fe:P ratios
 364 measured by ICP-MS were not significantly different between 100% OL and ACM treatments,
 365 suggesting the diatom could access the same amount of Fe from the precipitated Fe(III) in the
 366 OL as from the soluble (EDTA-chelated) Fe(III) in the ACM culture medium ($p=0.56$; **Supp.**
 367 **Fig 1A**). These data demonstrate that even at extremely high concentrations, olivine dissolution
 368 products including trace metals were not toxic to these diatoms, but instead may provide sources
 369 of the essential nutrients iron and silicate to support their growth in nutrient replete conditions.

370
 371 *Coccolithophores*

372 It has been hypothesized that calcifying coccolithophores may benefit from an increase in
 373 alkalinity from olivine dissolution (Bach et al., 2019). In the OL dilution series, maximum
 374 growth rates for the coccolithophore *Emiliana* equivalent to those recorded in the ACM positive
 375 control medium were achieved at all added OL concentrations from 10% to 100% (p=0.36,0.92,

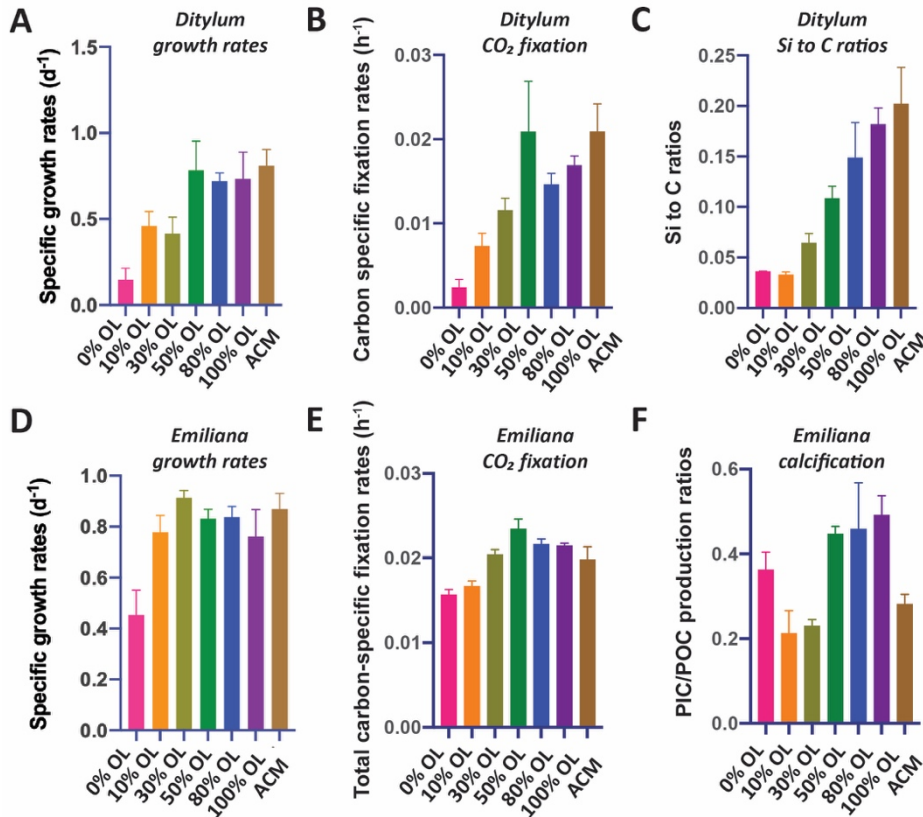


Fig 2. Effects of a dilution series of olivine leachate on growth and physiology of a marine diatom and coccolithophore. The diatom *Ditylum brightwellii* and the coccolithophore *Emiliana huxleyi* were grown across a range of dilutions of the olivine leachate (OL, 0-100%), and in the positive control medium (ACM). Shown are: **A)** Cell-specific growth rates (d⁻¹), **B)** Carbon-specific fixation rates (hr⁻¹) and **C)** Si:C ratios (mol Silicon: mol Carbon) of *Ditylum brightwellii*, and: **D)** Cell-specific growth rates (d⁻¹), **E)** Carbon-specific fixation rates (hr⁻¹), and **F)** PIC/POC production ratios (calcification production rate/organic carbon fixation rate, unitless) of *Emiliana huxleyi* in the same OL and ACM treatments. Y-axis values represent the means and error bars are the standard deviations of biological triplicate cultures for each treatment. Relative to the ACM positive control, significant differences in OL treatments are indicated by * = p < 0.05; ** = p < 0.01; *** = p < 0.001; **** = p < 0.0001.

407 **Fig. 2E).**

408 Particulate inorganic carbon to particulate organic carbon production ratios (PIC:POC production
 409 ratios) were significantly higher at OL levels of 50-100% than in the ACM positive controls
 410 (p=0.009, 0.005, 0.001, **Fig. 2F**), possibly due to enhanced alkalinity in the high OL
 411 concentration treatments. PIC:POC production ratios were elevated in the 0% OL treatment

0.96,
 0.98,0.26); the
 only
 significantly
 lower rate was
 at 0% OL
 (p<0.0001, **Fig.
 2D**). POC
 production
 (CO₂ fixation)
 rates were
 significantly
 reduced relative
 to the ACM in
 the 0%
 (p=0.0002) and
 10% (p=0.002)
 treatments; but
 in all higher OL
 concentrations,
 primary
 production
 increased to
 levels that were
 the same as or
 higher than the
 ACM control
 (30% p=0.99,
 50% p=0.04,
 80% p=0.29,
 100% p=0.45,

412 relative to those in the 10% and 30% OL treatments due to CO₂ fixation rates being reduced
 413 more than PIC fixation rates in this treatment, but in none of these treatments was this parameter
 414 significantly different from the ACM control (p=0.30,0.45,0.70, **Fig. 2F**).

415 An independent set of basic two-treatment experiments with the coccolithophore (ACM
 416 versus 100% OL, **Supp. Fig 2**) supported the results of the dilution series experiments shown in
 417 **Fig. 2**. *Emiliana* specific growth rates were slightly higher in the OL than in the ACM (p =
 418 0.05), while cellular particulate inorganic:particulate organic carbon ratios (PIC:POC, mol:mol)
 419 were not significantly different in the two treatments (p= 0.08, **Supp. Fig. 2A**). Likewise, both
 420 POC-specific fixation rates (p=0.04; TC h⁻¹) and PIC:POC production ratios were slightly higher

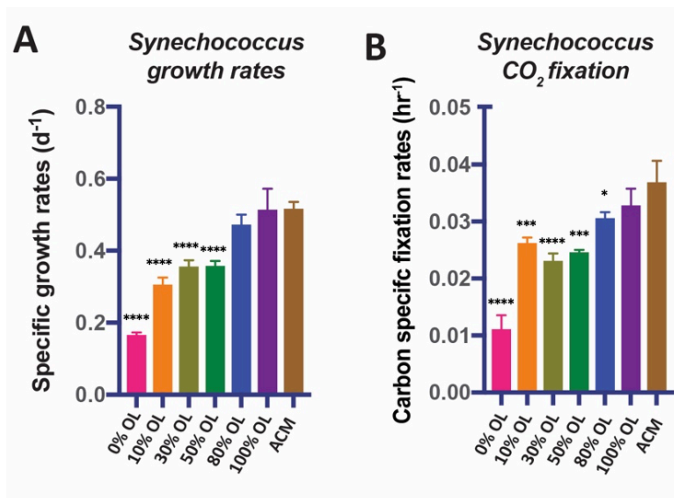


Fig 3. Effects of a dilution series of olivine leachate on growth and CO₂ fixation of a marine cyanobacterium. The unicellular picocyanobacterium *Synechococcus* sp. was grown across a range of dilutions of the olivine leachate (OL, 0-100%), and in the positive control medium (ACM). Shown are: **A**) Cell-specific growth rates (d⁻¹) and **B**) Carbon-specific fixation rates (hr⁻¹). Values represent the means and error bars are the standard deviations of triplicate cultures for each treatment. Relative to the ACM positive control, significant differences in OL treatments are indicated by * = p < 0.05; ** = p < 0.01; *** = p < 0.001; **** = p < 0.0001.

443

444 and CO₂ fixation rates (**Fig. 3B**) across the range of OL levels, similar to those of the eukaryotic
 445 algae. Both growth rates and carbon fixation rates were the same in the 100% OL treatment as in
 446 the ACM positive control treatment (p=0.94; p=0.46). ICP-MS measurements of *Synechococcus*
 447 cellular Fe:P ratios across a range of OL levels (0-100%) showed that this isolate accumulated
 448 much less Fe in the 0% OL than in the ACM treatment (p=0.02), but in all treatments with added
 449 OL, Fe:P ratios were the same as (10%. p=0.99, 30% 0.30, 50% 0.13, 100% 0.17) or higher than
 450 (80% p=0.01) than the ACM values (**Supp. Fig. 1B**). As with the eukaryotic phytoplankton

in the OL than in the ACM
 treatments (p=0.05, **Supp. Fig. 2B**).
 Like the diatoms, these data
 demonstrate that olivine dissolution
 products are also not toxic to this
 common coccolithophore species,
 and that enhanced alkalinity may
 support marginally higher growth
 rates under nutrient replete
 conditions.

Cyanobacteria

Like diatoms and
 coccolithophores, cyanobacteria
 could benefit from olivine
 dissolution due to their relatively
 high Fe (Hutchins and Boyd, 2016)
 and Ni requirements (Dupont et al.,
 2008). The OL dilution series
 experiments using the widely
 distributed picocyanobacterium
Synechococcus showed positive
 responses in growth rates (**Fig. 3A**)

451 tested, the synthetic OL provided a good source of Fe to support the growth of the
 452 picocyanobacterium.

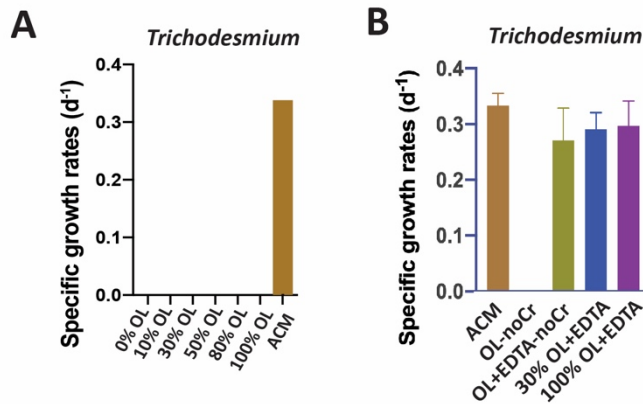


Fig 4. Effects of olivine leachate versus culture medium controls on growth of a colonial marine N₂-fixing cyanobacterium. Shown are **A**) Cell-specific growth rates (d⁻¹) of the colonial cyanobacterium *Trichodesmium erythraeum* across a range of dilutions of the olivine leachate (OL, 0-100%) and in the positive control medium (ACM), and **B**) Cell-specific growth rates (d⁻¹) of *Trichodesmium* in two concentrations of OL (30% and 100%) with the synthetic metal chelator EDTA, and in OL without Cr or EDTA, and in OL without Cr but plus EDTA, all versus ACM. Unless growth rates were zero, relative to the ACM positive control, significant differences in OL treatments are indicated by * = p < 0.05; ** = p < 0.01; *** = p < 0.001; **** = p < 0.0001.

476 more Fe than virtually any other phytoplankton species (Hutchins and Sañudo-Wilhelmy, 2021),
 477 and the OL was the only source of Fe provided in our experiments. Fe(II) released into seawater
 478 from olivine dissolution likely quickly oxidizes to Fe(III), which then precipitates and becomes
 479 insoluble at the elevated concentrations in our OL (Manck et al., 2022). This could render it
 480 biologically unavailable to the cellular Fe uptake systems of some species. We deliberately
 481 designed our OL to replicate this oxidation/precipitation process, and as expected observed
 482 visible reddish-brown amorphous colloidal Fe precipitates on the bottom of the growth flasks for
 483 all synthetic OL treatments. It is possible that other metals including Ni may have co-precipitated
 484 with the iron, as has been documented in other aquatic systems (Laxen 1985). If so, this would
 485 lower dissolved Ni levels, a process that could also occur during olivine deployments in the
 486 ocean.

487 Accordingly, we designed another set of experiments to test for both lack of Fe
 488 bioavailability and specific sensitivity to Cr, as has been done in previous cyanobacterial studies
 489 (Kiran et al., 2016). To do this, we formulated several variants of the olivine leachate: 1) normal
 490 OL (100% concentration), 2) OL (100% concentration) with a synthetic ligand (EDTA) that

In striking contrast to the eukaryotic algae and the non-diazotrophic (i.e., non-N₂-fixing) picocyanobacterium *Synechococcus*, the N₂-fixing cyanobacterium *Trichodesmium* could not grow at any concentration of OL tested (**Fig. 4A**). One possible explanation for this lack of growth is toxic effects by one of the trace metal components of the OL. We hypothesized that added levels of Ni and Co are unlikely to be toxic, as these nutrient metals have been found to be relatively non-toxic to many phytoplankton at similar environmental concentrations (Guo et al., 2022; Karthikeyan et al., 2019; Panneerselvam et al., 2018). Hence, we hypothesized that Cr toxicity should be considered as a likely possible scenario (Frey et al., 1983; Kiran et al., 2016). Another possibility is that *Trichodesmium* did not experience toxic effects but instead was unable to access Fe from OL. This N₂-fixer requires

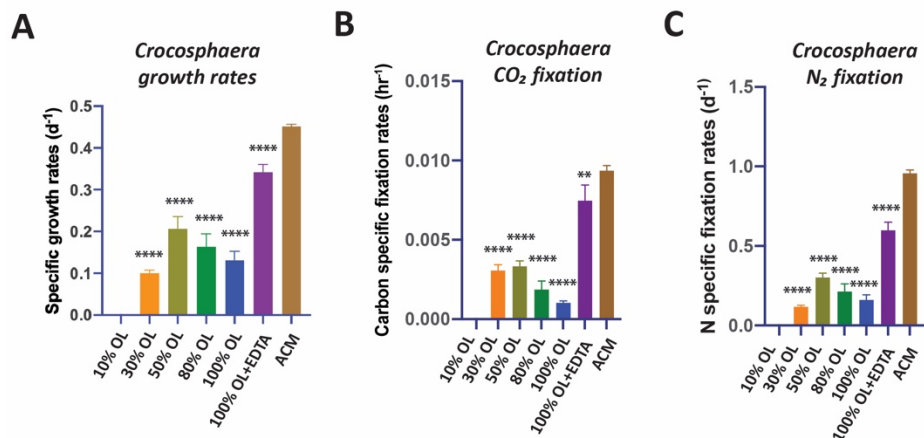


Fig 5. Effects of olivine leachate dilution series versus culture medium controls on the physiology of a unicellular marine N₂-fixing cyanobacterium.

A) Cell-specific growth rates (d⁻¹), B) Carbon-specific fixation rates (hr⁻¹), and C) N-specific fixation rates (day⁻¹) of the unicellular cyanobacterium *Crocospaera watsonii* grown across a range of dilutions of the olivine leachate (OL, 0-100%), in 100% OL plus EDTA (OL+EDTA), and in the positive control medium (ACM). Values represent the means and error bars are the standard deviations of triplicate cultures for each treatment. Relative to the ACM positive control, significant differences in OL treatments are indicated by * = p < 0.05; ** = p < 0.01; *** = p < 0.001; **** = p < 0.0001.

solubilizes Fe(III), and thus makes it broadly bioavailable (OL+EDTA), 3) OL (100% concentration) but with no Cr (OL-noCr), 4) and OL (100% concentration) but with no Cr and with EDTA (OL+EDTA-noCr) (Fig. 4B). *Trichodesmium* also could not grow in the OL medium without added Cr (OL-noCR, Fig. 4B), demonstrating

512 that the lack of growth observed in OL was not due to Cr toxicity. However, growth recovered to
 513 the same levels as in the ACM in all three treatments where EDTA was added (30%OL+EDTA
 514 p=0.62, 100%OL+EDTA p=0.84, 100%OL+EDTA-noCr p=0.30) to the leachate (Fig. 4B).
 515 Together, these results suggest that poor bioavailability of the precipitated Fe(III) (and not Cr
 516 toxicity) was the likely cause for *Trichodesmium*'s inability to grow in the unmodified OL.

517 OL also reduced the growth rates of the unicellular N₂-fixing cyanobacterium
 518 *Crocospaera*, although not to the same extent as for *Trichodesmium*, which didn't grow at all
 519 without the addition of EDTA. *Crocospaera* exhibited no growth at 0% OL, likely due to
 520 severe Fe limitation. From 10% to 100% OL, growth rates were 22-44% of those in ACM
 521 (p<0.001), and growth partially recovered in 100% OL+EDTA to 76% of rates in ACM
 522 (p<0.0001, Fig. 5A). Results were very similar for CO₂ fixation rates and N₂-fixation rates in
 523 OL, which were severely reduced by 64-100% (carbon fixation, p<0.0001) and 69-88% (N₂
 524 fixation, p<0.0001) relative to ACM in all OL treatments, but reached maximum values of 80%
 525 (p=0.002) and 63% (p<0.0001) of ACM treatment rates, respectively, when EDTA was added to
 526 the OL (Fig. 5B,C). This suggests that oxidized Fe from OL was not effectively utilized to
 527 support growth for either of the two N₂-fixing cyanobacteria tested, in contrast to the diatoms,
 528 coccolithophores, and *Synechococcus*. Their growth recovery after EDTA additions indicates
 529 that the other trace metals Cr, Ni, and Co in the olivine leachate were likely not toxic, even at
 530 extremely high concentrations. Interestingly, unlike *Trichodesmium* which could not grow at all

511

531 on OL alone but recovered fully upon EDTA additions, *Crocospaera* could still grow at lower
532 rates on OL but could not grow as fast upon EDTA additions as in ACM. Future experiments are
533 needed to understand these differences in species-specific responses between these two N₂-
534 fixers. Taken together, these data suggest that when olivine dissolves in seawater, it is unlikely to
535 provide a readily bioavailable Fe source to diazotrophic cyanobacteria, although this does not
536 preclude them obtaining Fe from their usual natural sources such as other sediments, rivers, dust
537 inputs etc. Thus, it seems likely that olivine may have negligible or no effect (positive or
538 negative) on the physiology of these cyanobacteria, although further work will be needed to put
539 these results into a more realistic ecological context to understand the full responses of N₂ fixing
540 cyanobacteria to olivine dissolution.

541

542 *Diatom/Coccolithophore Competitive Co-culture*

543 Results of the co-culture, or competition, experiment with the diatom *Ditylum*
544 *brightwellii* and the coccolithophore *Emiliana huxleyi* are shown in **Fig. 6**. Unlike the semi-
545 continuous experiments shown in the previous figures, this experiment used closed-system
546 “batch” culturing methods in order to assess and compare effects on relative biomass
547 accumulation by each species over time. OL (100% concentration) supported growth of both the
548 diatom (**Fig. 6A**) and the coccolithophore (**Fig. 6B**) in mixed culture, and biomass was very
549 similar for both species between the OL and ACM treatments throughout most of the
550 experiment. However, cell yields were higher in the ACM at the final timepoint for the diatom (p
551 = 0.009, **Fig. 6A**). Final cell counts were also higher in the ACM for the coccolithophore, but
552 this difference was not significant ($p = 0.31$; **Fig. 6B**). Similar trends were observed when diatom
553 biomass was estimated as biogenic silica (BSi, **Fig. 6C**, $p = 0.002$) and when coccolithophore
554 biomass was assessed as calcite or particulate inorganic carbon (PIC, **Fig. 6D**, $p = 0.04$). For the
555 diatom, OL supported growth rates similar to those in the ACM treatment during the first half of
556 the experiment (**Fig. 6A,C; Supp. Fig. 3A**). Growth rates were also similar in the OL and ACM
557 mediums for the coccolithophore (**Fig. 6B,D; Supp. Fig. 3B**). Hence, both phytoplankton
558 species were able to grow similarly well in co-culture, where neither exhibited any strong
559 competitive advantage over the other.

560

561

562

563

564

565

566

567

568

569

570

571 **Discussion**

572

573

574

575

In general, we observed no toxic effects from our simulated olivine dissolution products even at extremely high concentrations across all the phytoplankton species tested, consistent with other recent observations examining OAE scenarios (Gately et al., 2023) and trace metals (Guo et al., 2022).

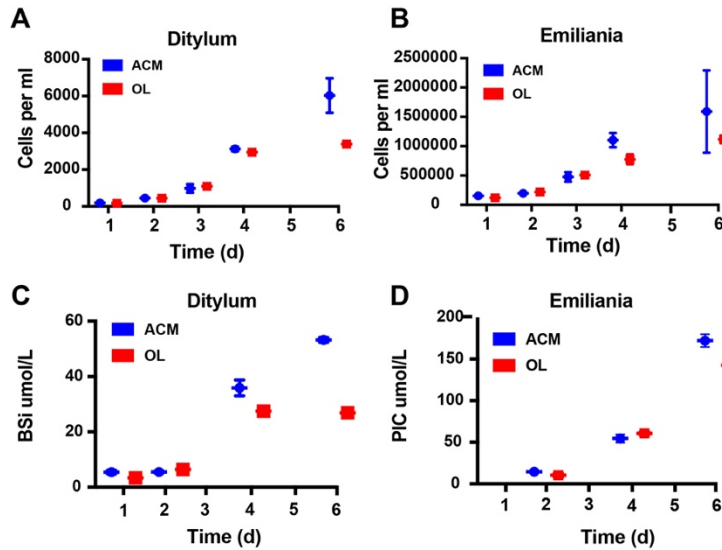


Fig. 6. Effects of olivine leachate versus culture medium controls on growth competition and biomineralization during co-culture of a diatom and a coccolithophore. Shown are 5-day growth curves (cells mL^{-1}) for **A**) the diatom *Ditylum brightwellii* and **B**) the coccolithophore *Emiliana huxleyi* in mixed cultures grown in olivine leachate (OL, red symbols) and positive control medium (ACM, blue symbols). Also shown are **C**) Biogenic silica (BSi, $\mu\text{mol L}^{-1}$), a proxy for diatom biomass, and **D**) Calcite or particulate inorganic carbon (PIC, $\mu\text{mol L}^{-1}$), a proxy for coccolithophore biomass, in the OL and ACM treatments in the same growth competition experiment. Values represent the means and error bars are the standard deviations of triplicate cultures for each treatment.

601

602

603

604

605

606

607

608

609

relative to the total dissolved Ni pool. Although broad negative effects of enhanced Ni concentrations were not observed across taxa, Guo observed some species-specific responses across variations in (0-100 μM) EDTA and Ni (0-50 μM) concentrations, indicating that specific phytoplankton groups are impacted differently depending on the chemical species in the total dissolved Ni pools and/or the concentration and type of organic ligands in seawater. Our results are generally consistent with their overall findings, as the phytoplankton groups tested here did not exhibit negative effects upon elevated exposure to Ni with (e.g., ACM) and without added EDTA (e.g., OL), suggesting that Ni was not toxic irrespective of the concentration of different Ni species in the dissolved pool or that of the Ni^{2+} ion. However, our experiments were not

particularly focused on exposing 11 phytoplankton groups to elevated Ni concentrations and did not observe strong effects across these taxa. Although it is unknown what chemical species of dissolved Ni primarily influence phytoplankton physiology, most studies indicate that phytoplankton primarily interact with free Ni^{2+} ions but are not particularly sensitive to the total dissolved Ni concentration (Guo et al., 2022). Guo et al. (2022) and our study used the same Ni-containing compound, NiCl_2 , as a source of Ni^{2+} . Guo et al. also used the same base Aquil control medium as our ACM. ACM contains EDTA that binds with metal ions like Ni to improve their dissolution, which subsequently lowers the free Ni ion concentrations (e.g., Ni^{2+})

610 designed to test for taxon-specific differences in responses to specific Ni species or variations in
611 EDTA concentrations.

612 The two diatoms were able to use synthetic OL-derived Si and Fe to support near-
613 maximum growth rates and carbon fixation rates, as well as robust silica frustule development
614 (as assessed by cellular Si:C ratios); both of these nutrients can frequently limit diatom growth in
615 various parts of the ocean (Tréguer et al., 2018; Hutchins and Boyd, 2016). OL-derived
616 alkalinity and iron increases also supported growth of the tested coccolithophore, consistent with
617 previous observations showing increases in red algae calcification (Gore et al., 2019) and net reef
618 calcification calcifying corals (Albright et al., 2016) in response to OAE. Similarly, a
619 representative of the globally distributed, picocyanobacterium *Synechococcus* increased its
620 growth and carbon fixation rates as OL concentrations increased. Although OL could not support
621 *Trichodesmium* and *Crocospaera* growth due to their inability to use Fe(III), olivine dissolution
622 products were not observed to be toxic. Their inability to use Fe(III) is a neutral effect due to
623 other sources of bioavailable Fe in the water column (Hutchins and Boyd, 2016).

624 Thus, these results using 6 model species suggest that many phytoplankton species may
625 not be negatively impacted by even high levels of elements derived from olivine dissolution, and
626 that some olivine dissolution products may support their growth, primary productivity, and
627 biomineralization when OL is available at high enough concentrations in certain environmental
628 conditions. For example, it is important to note that potential growth benefits to phytoplankton *in*
629 *situ* will also depend on ambient concentrations of other important nutrients, such as nitrogen (N)
630 and phosphorus (P). Our cultures contained an abundance of other required nutrients, thus
631 enabling phytoplankton to take advantage of dissolution products for growth (e.g., Si, Fe,
632 alkalinity). However, if nutrients like N and P are primarily limiting in natural environments,
633 then olivine dissolution products are not expected to have any growth effect. In addition, these
634 cultures represent closed systems that do not allow olivine products to be diluted with fresh
635 seawater. In natural settings, advection in both sediment porewaters (Reimers et al., 2004) and
636 the water column (He and Tyka, 2022) will lead to short residence times, thereby rapidly diluting
637 olivine dissolution products. Hence, these physical dynamics will prevent high concentrations of
638 olivine dissolution products from accumulating in seawater in coastal systems. Thus, even the
639 most dilute leachate treatment in this study is likely more concentrated than the anticipated
640 concentrations of olivine dissolution products expected under field conditions. It is important to
641 note though that our experiments focused on physiological responses, while further work will be
642 needed to explore the possibility of indirect effects on important ecological factors such as
643 predation or competition. Further research will also be needed to test for direct and indirect
644 effects using other species of phytoplankton not examined here and belonging to other important
645 functional groups.

646 Bach et al. (2019) (Bach et al., 2019) hypothesized that under nutrient-limited conditions,
647 silicate, iron and nickel releases from marine applications of silicate minerals like olivine might
648 particularly benefit diatoms and cyanobacteria, as these groups have especially high
649 requirements for one or more of these nutrients. Thus, they expected that olivine applications

650 might produce a “Greener” ocean. They also suggested that adding minerals derived from
651 CaCO_3^- (such as quicklime applications) would particularly favor coccolithophores, due to
652 rapidly enhanced seawater alkalinity. This outcome would produce a “Whiter” ocean (the color
653 of coccolithophore calcite). Although we did not test CaCO_3^- derivatives, our results with
654 nutrient-replete synthetic OL seem to represent a “Green and White” ocean scenario, since in
655 individual experiments diatoms, picocyanobacteria, and coccolithophores all responded
656 positively to OL at the relatively elevated levels applied in our experiments. This conclusion is
657 further supported by the results of our nutrient replete diatom/coccolithophore co-culture
658 experiment, which showed that OL stimulated both species simultaneously rather than conferring
659 a competitive advantage on one or the other. This suggests that in the ocean, competitive
660 outcomes between diatoms and coccolithophores may not be affected by olivine dissolution
661 under nutrient-replete conditions, although we did not test this under nutrient-limited conditions
662 that are commonly encountered by phytoplankton in nature.

663 Iron in olivine minerals is present as reduced Fe(II), and we added it in this form to our
664 synthetic OL. However, when Fe(II) dissolves in oxic seawater, it quickly (within minutes)
665 oxidizes to highly insoluble Fe(III), which precipitates out as amorphous iron hydroxides
666 (Millero et al., 1987). Clearly, in our experiments this oxidized particulate iron must have been
667 available to the species that showed growth enhancement with OL, since no other iron source
668 was provided in the seawater growth medium. In accordance with their well-studied reductive Fe
669 uptake systems (Morrissey and Bowler, 2012), there is evidence that diatoms can access Fe to
670 some degree from freshly precipitated amorphous colloidal Fe hydroxides (like those in our
671 experiments), although the bioavailability of Fe precipitates declines quickly as the hydroxides
672 age and acquire a more crystalline structure (Yoshida et al., 2006). Alternately, the precipitated
673 Fe in our experiments could have become available to the phytoplankton ferric reductases via
674 solubilization by siderophores produced by bacteria in our non-axenic cultures (Coale et al.,
675 2019). In some cases diatoms, can also potentially take up Fe through endocytosis (Kazamia et
676 al., 2018).

677 The responses of the two N_2 -fixing cyanobacteria were in striking contrast to those of the
678 other three phytoplankton groups tested. These diazotrophs were either unable to grow in our
679 artificial OL at all (*Trichodesmium*), or could only grow to a very limited degree
680 (*Crocospaera*). However, our results with experimental additions of the artificial iron chelator
681 EDTA (ethylene diamine tetra acetic acid) suggest that other mechanisms may enable iron
682 bioavailability. For example, previous research has suggested that *Trichodesmium* cannot
683 directly access particulate Fe(III) forms, but likely relies on bacteria residing on and in natural
684 colonies to produce siderophores, which then solubilize particulate Fe(III) sources and make
685 them bioavailable (Rubin et al., 2011; Lee et al., 2018). Since cultured *Trichodesmium* such as
686 ours typically do not produce colonies, but grow instead as individual filaments of cells, cultures
687 of this diazotroph are likely deficient in many of these iron-acquiring microbial symbionts
688 (Rubin et al., 2011). The iron uptake systems of *Crocospaera* have been less well-
689 characterized, but like *Trichodesmium*, molecular studies suggest this unicellular diazotroph

690 lacks the genetic capacity to produce endogenous siderophores (Shi et al., 2010; Yang et al.,
691 2022). Our results show that when we add the artificial iron chelator EDTA (which substitutes
692 for ligands produced by the missing bacteria in cultures), the synthetic OL supports near-
693 maximum growth of both diazotrophs. Thus, reduced growth rates of these cyanobacteria in OL
694 without EDTA appear to be due to severe iron limitation, not toxicity of any OL component. In
695 our experiments the cells were forced to grow on OL as a sole source of iron, but in coastal
696 ecosystems where olivine deployments would occur, there are typically many other natural
697 sources of iron to support algal growth (Capone and Hutchins, 2013; Hutchins and Boyd, 2016).
698 In nature, *Trichodesmium* is also likely to occur mostly as colonies, and so may have access to
699 additional siderophore-bound iron, including from both naturally occurring supplies as well as
700 potentially from any oceanic olivine applications. Thus, changes in the iron nutritional status of
701 N₂ fixers due to olivine additions in-situ may not occur in the real ocean.

702 While the reduced growth rates of the diazotrophs on our synthetic OL appears to be due
703 to iron limitation, our experiments also shed light on potential effects of other trace metals
704 present in the formulation. Of the metals found in our synthetic OL, Ni and Co are considered
705 nutrient elements with relatively low toxicity; in fact, the concentrations added even in our
706 maximum dosage experiments were well below those that have been reported to be toxic to
707 phytoplankton (Karthikeyan et al., 2019; Vink and Knops, 2023). However, Cr has the potential
708 to be biologically problematic. Cr(III) found in olivine is relatively insoluble, so in this form it is
709 probably not a major source of exposure for planktonic organisms. However, if it oxidizes to
710 Cr(VI), it becomes much more soluble, and thus more bioavailable and potentially toxic. Cr(III)
711 oxidation is thermodynamically unfavorable, but can be facilitated by borate ions always present
712 in seawater, or by the presence of biologically or photochemically-produced oxidants like H₂O₂
713 (Pettine et al., 1991), and by naturally occurring manganese oxides (Weijden and Reith, 1982).
714 For these reasons, following the principle of “worst case scenario”, we used a soluble Cr(VI) salt
715 in our synthetic OL formulation. Despite this, we found that the presence or absence of the
716 relatively elevated levels of dissolved Cr(VI) in our regular synthetic OL did not make any
717 difference to the growth of *Trichodesmium* or the other tested phytoplankton species.
718 Particularly, because synthetic OL stimulated near-maximum growth rates in the diatoms,
719 coccolithophore and picocyanobacterium, we presume that the Cr(VI) additions did not
720 adversely affect these groups either.

721 The goal of this work was to test both extreme levels and simultaneous exposure of
722 multiple, biologically important olivine dissolution products that could influence microbial
723 physiology in order to identify thresholds and response curves. Accordingly, our experiments
724 focused on determining acute effects of high concentrations of olivine dissolution products. In
725 general, they suggest that negative impacts may be few even for large olivine deployments, given
726 the high concentrations of tested olivine dissolution products. Because these microplankton serve
727 as important links to higher trophic levels, these data suggest minimal long-term impacts from
728 olivine dissolution on ecosystem services. Future research directions may include longer term
729 experiments with prokaryotes and natural microbial communities to expand our understanding of

730 olivine exposure on important taxa that help drive biogeochemical cycling in the oceans,
731 particularly experiments to test for ecological effects on processes like competition and trophic
732 interactions at the community and ecosystem levels. Similar experiments can also be conducted
733 except with other OAE feedstocks harboring different chemical compositions and more rapid
734 dissolution timescales (Renforth and Henderson, 2017). Future studies can also focus on
735 determining how biological processes like photosynthesis, respiration, and organic ligand
736 production could influence olivine dissolution kinetics and their impacts on carbon dioxide
737 removal.

738
739 **Data Availability.** All data and parameters can be found at <https://zenodo.org/record/8157750>.

740
741 **Author contribution:** D.A.H., F.-X.F., S.J.R., and N.G.W. designed the research; D.A.H., F.-
742 X.F., S.-C.Y, and S.G.J. performed the research. D.A.H., F.-X.F., S.-C.Y, N.G.W., and S.G.J.
743 analyzed the data. D.A.H., F.-X.F., S.-C.Y, N.G.W., S.J.R., M.G.A., and S.G.J. wrote the paper.

744
745 **Competing interests:** Authors D.A.H. and F.-X.F. received research funding from Vesta, PBC.
746 N.G.W., M.G.A., and S.J.R. are full time employees at Vesta, PBC.

747
748

749

750

751

752

753

754

755

756

757

758

759

760

761

References

762 Albright, R., Caldeira, L., Hosfelt, J., Kwiatkowski, L., Maclaren, J. K., Mason, B. M.,
763 Nebuchina, Y., Ninokawa, A., Pongratz, J., Ricke, K. L., Rivlin, T., Schneider, K., Sesboüé, M.,
764 Shamberger, K., Silverman, J., Wolfe, K., Zhu, K., and Caldeira, K.: Reversal of ocean
765 acidification enhances net coral reef calcification, *Nature*, 531, 362–365,
766 <https://doi.org/10.1038/nature17155>, 2016.

767

768 Bach, L. T., Gill, S. J., Rickaby, R. E. M., Gore, S., and Renforth, P.: CO₂ Removal With
769 Enhanced Weathering and Ocean Alkalinity Enhancement: Potential Risks and Co-benefits for
770 Marine Pelagic Ecosystems, *Frontiers in Climate*, 1–21,
771 <https://doi.org/10.3389/fclim.2019.00007>, 2019.

772

773 Beerling, D. J., Kantzas, E. P., Lomas, M. R., Wade, P., Eufrazio, R. M., Renforth, P., Sarkar, B.,
774 Andrews, M. G., James, R. H., Pearce, C. R., Mercure, J.-F., Pollitt, H., Holden, P. B., Edwards,
775 N. R., Khanna, M., Koh, L., Quegan, S., Pidgeon, N. F., Janssens, I. A., Hansen, J., and Banwart,
776 S. A.: Potential for large-scale CO₂ removal via enhanced rock weathering with croplands,
777 *Nature*, 1–20, <https://doi.org/10.1038/s41586-020-2448-9>, 2021.

778

779 Bertrand, E. M., Allen, A. E., Dupont, C. L., Norden-Krichmar, T. M., Bai, J., Valas, R., and
780 Saito, M. A.: Influence of cobalamin scarcity on diatom molecular physiology and identification
781 of a cobalamin acquisition protein, *Proceedings of the National Academy of Sciences*, E1762–
782 E1771, <https://doi.org/10.1073/pnas.1201731109/-/dcsupplemental>, 2012.

783

784 Brzezinski, M. A.: THE Si:C:N RATIO OF MARINE DIATOMS: INTERSPECIFIC
785 VARIABILITY AND THE EFFECT OF SOME ENVIRONMENTAL VARIABLES, *J Phycol*,
786 21, 347–357, <https://doi.org/10.1111/j.0022-3646.1985.00347.x>, 1985.

787

788 Capone, D. G. and Hutchins, D. A.: Microbial biogeochemistry of coastal upwelling regimes in a
789 changing ocean, *Nat Geosci*, 6, 711–717, <https://doi.org/10.1038/ngeo1916>, 2013.

790 Caserini, S., Storni, N., and Grosso, M.: The Availability of Limestone and Other Raw Materials
791 for Ocean Alkalinity Enhancement, *Glob. Biogeochem. Cycles*, 36,
792 <https://doi.org/10.1029/2021gb007246>, 2022.

793 Coale, T. H., Moosburner, M., Horák, A., Oborník, M., Barbeau, K. A., and Allen, A. E.:
794 Reduction-dependent siderophore assimilation in a model pennate diatom, *Proceedings of the*
795 *National Academy of Sciences*, 1–9, <https://doi.org/10.1073/pnas.1907234116>, 2019.

796 Dupont, C. L., Barbeau, K., and Palenik, B.: Ni Uptake and Limitation in Marine *Synechococcus*
797 Strains, *Appl Environ Microb*, 74, 23–31, <https://doi.org/10.1128/aem.01007-07>, 2008.

798

799 Field, C., Behrenfeld, M., Randerson, J., and Falkowski, P.: Primary production of the biosphere:
800 integrating terrestrial and oceanic components, *Science*, 281, 237–240, 1998.

801

802 Flipkens, G., Blust, R., and Town, R. M.: Deriving Nickel (Ni(II)) and Chromium (Cr(III))
803 Based Environmentally Safe Olivine Guidelines for Coastal Enhanced Silicate Weathering,
804 *Environ Sci Technol*, 55, 12362–12371, <https://doi.org/10.1021/acs.est.1c02974>, 2021.

805

806 Frey, B. E., Riedel, G. F., Bass, A. E., and Small, L. F.: Sensitivity of estuarine phytoplankton to
807 hexavalent chromium, *Estuar Coast Shelf Sci*, 17, 181–187, [https://doi.org/10.1016/0272-](https://doi.org/10.1016/0272-7714(83)90062-8)
808 [7714\(83\)90062-8](https://doi.org/10.1016/0272-7714(83)90062-8), 1983.

809

810 Fu, F., Zhang, Y., Bell, P. R. F., and Hutchins, D. A.: PHOSPHATE UPTAKE AND GROWTH
811 KINETICS OF *TRICHODESMIUM* (CYANOBACTERIA) ISOLATES FROM THE NORTH
812 ATLANTIC OCEAN AND THE GREAT BARRIER REEF, AUSTRALIA1, *J Phycol*, 41, 62–
813 73, <https://doi.org/10.1111/j.1529-8817.2005.04063.x>, 2005.

814

815 Fu, F., Tschitschko, B., Hutchins, D. A., Larsson, M. E., Baker, K. G., McInnes, A., Kahlke, T.,
816 Verma, A., Murray, S. A., and Doblin, M. A.: Temperature variability interacts with mean
817 temperature to influence the predictability of microbial phenotypes, *Global Change Biol*, 28,
818 5741–5754, <https://doi.org/10.1111/gcb.16330>, 2022.

819

820 Fu, F. X., Yu, E., Garcia, N. S., Gale, J., Luo, Y., Webb, E. A., and Hutchins, D. A.: Differing
821 responses of marine N₂ fixers to warming and consequences for future diazotroph community
822 structure, *Aquatic Microbial Ecology*, 72, 33–46, <https://doi.org/10.3354/ame01683>, 2014.

823

824 Fu, F.-X., Mulholland, M. R., Garcia, N. S., Beck, A., Bernhardt, P. W., Warner, M. E., Sañudo-
825 Wilhelmy, S. A., and Hutchins, D. A.: Interactions between changing pCO₂, N₂ fixation, and Fe
826 limitation in the marine unicellular cyanobacterium *Crocospaera*, *Limnology and*
827 *Oceanography*, 53, 2472–2484, <https://doi.org/10.4319/lo.2008.53.6.2472>, 2008.

828 Gately, J. A., Kim, S. M., Jin, B., Brzezinski, M. A., and Iglesias-Rodriguez, M. D.:
829 Coccolithophores and diatoms resilient to ocean alkalinity enhancement: A glimpse of hope?,
830 *Sci. Adv.*, 9, eadg6066, <https://doi.org/10.1126/sciadv.adg6066>, 2023.

831 Gore, S., Renforth, P., and Perkins, R.: The potential environmental response to increasing ocean
832 alkalinity for negative emissions, *Mitig. Adapt. Strat. Glob. Chang.*, 24, 1191–1211,
833 <https://doi.org/10.1007/s11027-018-9830-z>, 2019.

834

835 Guo, J. A., Strzepek, R., Willis, A., Ferderer, A., and Bach, L. T.: Investigating the effect of
836 nickel concentration on phytoplankton growth to assess potential side-effects of ocean alkalinity
837 enhancement, *Biogeosciences*, 19, 3683–3697, <https://doi.org/10.5194/bg-19-3683-2022>, 2022.

838

839 Hartmann, J., West, A. J., Renforth, P., Köhler, P., Rocha, C. L. D. L., Wolf-Gladrow, D. A.,
840 Dürr, H. H., and Scheffran, J.: ENHANCED CHEMICAL WEATHERING AS A
841 GEOENGINEERING STRATEGY TO REDUCE ATMOSPHERIC CARBON DIOXIDE,
842 SUPPLY NUTRIENTS, AND MITIGATE OCEAN ACIDIFICATION, *Reviews of Geophysics*,
843 1–37, <https://doi.org/10.1002/rog.20004>, 2013.

844 Hauck, J., Köhler, P., Wolf-Gladrow, D., and Völker, C.: Iron fertilisation and century-scale
845 effects of open ocean dissolution of olivine in a simulated CO₂ removal experiment, *Environ.*
846 *Res. Lett.*, 11, 024007, <https://doi.org/10.1088/1748-9326/11/2/024007>, 2016.

847

848 Hawco, N. J., McIlvin, M. M., Bundy, R. M., Tagliabue, A., Goepfert, T. J., Moran, D. M.,
849 Valentin-Alvarado, L., DiTullio, G. R., and Saito, M. A.: Minimal cobalt metabolism in the
850 marine cyanobacterium *Prochlorococcus*, *Proc National Acad Sci*, 117, 15740–15747,
851 <https://doi.org/10.1073/pnas.2001393117>, 2020.

852

853 He, J. and Tyka, M. D.: Limits and CO₂ equilibration of near-coast alkalinity enhancement,
854 *Egusphere*, 2022, 1–26, <https://doi.org/10.5194/egusphere-2022-683>, 2022.

855

856 Hutchins, D. A. and Boyd, P. W.: Marine phytoplankton and the changing ocean iron cycle,
857 *nature climate change*, 6, 1072–1079, <https://doi.org/10.1038/nclimate3147>, 2016.

858

859 Hutchins, D. A. and Sañudo-Wilhelmy, S. A.: The Enzymology of Ocean Global Change, *Annu*
860 *Rev Mar Sci*, 14, 1–25, <https://doi.org/10.1146/annurev-marine-032221-084230>, 2021.

861

862 Hutchins, D. A., Fu, F.-X., Zhang, Y., Warner, M. E., Feng, Y., Portune, K., Bernhardt, P. W.,
863 and Mulholland, M. R.: CO₂ control of *Trichodesmium* N₂ fixation, photosynthesis, growth
864 rates, and elemental ratios: Implications for past, present, and future ocean biogeochemistry,
865 *Limnol Oceanogr*, 52, 1293–1304, <https://doi.org/10.4319/lo.2007.52.4.1293>, 2007.

866 IPCC: IPCC, 2022: Climate Change 2022: Mitigation of Climate Change. Contribution of
867 Working Group III to the Sixth Assessment Report of the Intergovernmental Panel on Climate
868 Change, *Popul. Dev. Rev.*, 48, 629–633, <https://doi.org/10.1017/9781009157926>, 2022.

869

870 Jiang, H.-B., Fu, F.-X., Rivero-Calle, S., Levine, N. M., Sañudo-Wilhelmy, S. A., Qu, P.-P.,
871 Wang, X.-W., Pinedo-Gonzalez, P., Zhu, Z., and Hutchins, D. A.: Ocean warming alleviates iron
872 limitation of marine nitrogen fixation, *Nat Clim Change*, 8, 709–712,
873 <https://doi.org/10.1038/s41558-018-0216-8>, 2018.

874

875 John, S. G., Kelly, R. L., Bian, X., Fu, F., Smith, M. I., Lanning, N. T., Liang, H., Pasquier, B.,
876 Seelen, E. A., Holzer, M., Wasylenki, L., Conway, T. M., Fitzsimmons, J. N., Hutchins, D. A.,
877 and Yang, S.-C.: The biogeochemical balance of oceanic nickel cycling, *Nat Geosci*, 15, 906–
878 912, <https://doi.org/10.1038/s41561-022-01045-7>, 2022.

879 John, S. G., Mendez, J., Moffett, J., and Adkins, J.: The flux of iron and iron isotopes from San
880 Pedro Basin sediments, *Geochim. Cosmochim. Acta*, 93, 14–29,
881 <https://doi.org/10.1016/j.gca.2012.06.003>, 2012.

882

883 Karthikeyan, P., Marigoudar, S. R., Nagarjuna, A., and Sharma, K. V.: Toxicity assessment of
884 cobalt and selenium on marine diatoms and copepods, *Environ Chem Ecotoxicol*, 1, 36–42,
885 doi.org/10.1016/j.enceco.2019.06.001, 2019.

886

887 Kazamia, E., Sutak, R., Paz-Yepes, J., Dorrell, R. G., Vieira, F. R. J., Mach, J., Morrissey, J.,
888 Leon, S., Lam, F., Pelletier, E., Camadro, J.-M., Bowler, C., and Lesuisse, E.: Endocytosis-
889 mediated siderophore uptake as a strategy for Fe acquisition in diatoms, *Sci Adv*, 4, eaar4536,
890 <https://doi.org/10.1126/sciadv.aar4536>, 2018.

891

892 Kiran, B., Rani, N., and Kaushik, A.: Environmental toxicity: Exposure and impact of chromium
893 on cyanobacterial species, *J Environ Chem Eng*, 4, 4137–4142,
894 <https://doi.org/10.1016/j.jece.2016.09.021>, 2016.

895

896 Kling, J. D., Kelly, K. J., Pei, S., Rynearson, T. A., and Hutchins, D. A.: Irradiance modulates
897 thermal niche in a previously undescribed low-light and cold-adapted nano-diatom, *Limnol*
898 *Oceanogr*, 66, 2266–2277, <https://doi.org/10.1002/lno.11752>, 2021.

899 Laxen D.P.H., 1985. Trace metal adsorption/coprecipitation on hydrous ferric oxide under
900 realistic conditions: The role of humic substances, *Water Research* 19(10): 1229-1236.

901
902 Lee, M. D., Webb, E. A., Walworth, N. G., Fu, F.-X., Held, N. A., Saito, M. A., and Hutchins,
903 D. A.: Transcriptional Activities of the Microbial Consortium Living with the Marine Nitrogen-
904 Fixing Cyanobacterium *Trichodesmium* Reveal Potential Roles in Community-Level Nitrogen
905 Cycling, *Applied and environmental microbiology*, 84, e02026-17–16,
906 <https://doi.org/10.1128/aem.02026-17>, 2018.

907
908 Manck, L. E., Park, J., Tully, B. J., Poire, A. M., Bundy, R. M., Dupont, C. L., and Barbeau, K.
909 A.: Petrobactin, a siderophore produced by *Alteromonas*, mediates community iron acquisition in
910 the global ocean, *Isme J*, 16, 358–369, <https://doi.org/10.1038/s41396-021-01065-y>, 2022.

911
912 Meysman, F. J. R. and Montserrat, F.: Negative CO₂ emissions via enhanced silicate weathering
913 in coastal environments, *Biol Letters*, 13, 20160905, <https://doi.org/10.1098/rsbl.2016.0905>,
914 2017.

915
916 Millero, F. J., Sotolongo, S., and Izaguirre, M.: The oxidation kinetics of Fe(II) in seawater,
917 *Geochim Cosmochim Ac*, 51, 793–801, [https://doi.org/10.1016/0016-7037\(87\)90093-7](https://doi.org/10.1016/0016-7037(87)90093-7), 1987.
918 Moran, M. A.: The global ocean microbiome, *Science*, 350, aac8455–aac8455,
919 <https://doi.org/10.1126/science.aac8455>, 2015.

920 Moran, M. A.: The global ocean microbiome, *Science*, 350, aac8455–aac8455,
921 <https://doi.org/10.1126/science.aac8455>, 2015.

922
923 Morrissey, J. M. and Bowler, C.: Iron utilization in marine cyanobacteria and eukaryotic algae,
924 *Frontiers in Microbiology*, 3, 1–13, <https://doi.org/10.3389/fmicb.2012.00043/abstract>, 2012.

925 Oelkers, E. H., Declercq, J., Saldi, G. D., Gislason, S. R., and Schott, J.: Olivine dissolution
926 rates: A critical review, *Chem Geol*, 500, 1–19, <https://doi.org/10.1016/j.chemgeo.2018.10.008>,
927 2018.

928
929 Paasche, E., Brubak, S., Skattebøl, S., Young, J. R., and Green, J. C.: Growth and calcification in
930 the coccolithophorid *Emiliana huxleyi* (Haptophyceae) at low salinities, *Phycologia*, 35, 394–
931 403, <https://doi.org/10.2216/i0031-8884-35-5-394.1>, 1996.

932
933 Panneerselvam, K., Marigoudar, S. R., and Dhandapani, M.: Toxicity of Nickel on the Selected
934 Species of Marine Diatoms and Copepods, *Bull. Environ. Contam. Toxicol.*, 100, 331–337,
935 <https://doi.org/10.1007/s00128-018-2279-7>, 2018.

936
937 Pettine, M., Millero, F. J., and Noce, T. L.: Chromium (III) interactions in seawater through its
938 oxidation kinetics, *Mar Chem*, 34, 29–46, [https://doi.org/10.1016/0304-4203\(91\)90012-1](https://doi.org/10.1016/0304-4203(91)90012-1), 1991.

939
940 Reimers, C. E., Stecher, H. A., Taghon, G. L., Fuller, C. M., Huettel, M., Rusch, A., Ryckelynck,
941 N., and Wild, C.: In situ measurements of advective solute transport in permeable shelf sands,
942 *Cont Shelf Res*, 24, 183–201, <https://doi.org/10.1016/j.csr.2003.10.005>, 2004.

943
944 Renforth, P. and Henderson, G.: Assessing ocean alkalinity for carbon sequestration, *Rev*
945 *Geophys*, 55, 636–674, <https://doi.org/10.1002/2016rg000533>, 2017.

946
947 Rimstidt, J. D., Brantley, S. L., and Olsen, A. A.: Systematic review of forsterite dissolution rate
948 data, *Geochim Cosmochim Acta*, 99, 159–178, <https://doi.org/10.1016/j.gca.2012.09.019>, 2012.

949 Rogelj, J., Popp, A., Calvin, K. V., Luderer, G., Emmerling, J., Gernaat, D., Fujimori, S.,
950 Strefler, J., Hasegawa, T., Marangoni, G., Krey, V., Kriegler, E., Riahi, K., Vuuren, D. P. van,
951 Doelman, J., Drouet, L., Edmonds, J., Fricko, O., Harmsen, M., Havlík, P., Humpenöder, F.,
952 Stehfest, E., and Tavoni, M.: Scenarios towards limiting global mean temperature increase below
953 1.5 °C, *Nat. Clim. Chang.*, 8, 325–332, <https://doi.org/10.1038/s41558-018-0091-3>, 2018.

954
955 Rubin, M., Berman-Frank, I., and Shaked, Y.: Dust- and mineral-iron utilization by the marine
956 dinitrogen-fixer *Trichodesmium*, *Nature Geoscience*, 4, 529–534,
957 <https://doi.org/10.1038/ngeo1181>, 2011.

958
959 Shi, T., Ilikchyan, I., Rabouille, S., and Zehr, J. P.: Genome-wide analysis of diel gene
960 expression in the unicellular N₂-fixing cyanobacterium *Crocospaera watsonii* WH 8501, *Isme*
961 *J*, 4, 621–632, <https://doi.org/10.1038/ismej.2009.148>, 2010.

962
963 Sunda, W. G. and Huntsman, S. A.: Cobalt and zinc interreplacement in marine phytoplankton:
964 Biological and geochemical implications, *Limnol Oceanogr*, 40, 1404–1417,
965 <https://doi.org/10.4319/lo.1995.40.8.1404>, 1995.

966
967 Sunda, W. G., Price, N. M., and Morel, F. M. M.: Trace Metal Ion Buffers and Their Use in
968 Culture Studies, *Algal Culturing Techniques*, 35–63, [https://doi.org/10.1016/b978-012088426-](https://doi.org/10.1016/b978-012088426-1/50005-6)
969 [1/50005-6](https://doi.org/10.1016/b978-012088426-1/50005-6), 2005.

970 Taylor, L. L., Quirk, J., Thorley, R. M. S., Kharecha, P. A., Hansen, J., Ridgwell, A., Lomas, M.
971 R., Banwart, S. A., and Beerling, D. J.: Enhanced weathering strategies for stabilizing climate
972 and averting ocean acidification, *Nat. Clim. Chang.*, 6, 402–406,
973 <https://doi.org/10.1038/nclimate2882>, 2016.

974

975 Tovar-Sanchez, A., Sañudo-Wilhelmy, S. A., Garcia-Vargas, M., Weaver, R. S., Popels, L. C.,
976 and Hutchins, D. A.: A trace metal clean reagent to remove surface-bound iron from marine
977 phytoplankton, *Mar Chem*, 82, 91–99, [https://doi.org/10.1016/s0304-4203\(03\)00054-9](https://doi.org/10.1016/s0304-4203(03)00054-9), 2003.

978

979 Tréguer, P., Bowler, C., Moriceau, B., Dutkiewicz, S., Gehlen, M., Aumont, O., Bittner, L.,
980 Dugdale, R., Finkel, Z., Iudicone, D., Jahn, O., Guidi, L., Lasbleiz, M., Leblanc, K., Levy, M.,
981 and Pondaven, P.: Influence of diatom diversity on the ocean biological carbon pump, *Nat*
982 *Geosci*, 11, 27–37, <https://doi.org/10.1038/s41561-017-0028-x>, 2018.

983

984 Vink, J. P. M. and Knops, P.: Size-Fractionated Weathering of Olivine, Its CO₂-Sequestration
985 Rate, and Ecotoxicological Risk Assessment of Nickel Release, *Mineral-basel*, 13, 235,
986 <https://doi.org/10.3390/min13020235>, 2023.

987

988 Weijden, C. H. V. D. and Reith, M.: Chromium(III) — chromium(VI) interconversions in
989 seawater, *Mar Chem*, 11, 565–572, [https://doi.org/10.1016/0304-4203\(82\)90003-2](https://doi.org/10.1016/0304-4203(82)90003-2), 1982.

990 Welschmeyer, N. A.: Fluorometric analysis of chlorophyll a in the presence of chlorophyll b and
991 pheopigments, *Limnol Oceanogr*, 39, 1985–1992, <https://doi.org/10.4319/lo.1994.39.8.1985>,
992 1994.

993

994 Yamamoto, T., Goto, I., Kawaguchi, O., Minagawa, K., Ariyoshi, E., and Matsuda, O.:
995 Phytoremediation of shallow organically enriched marine sediments using benthic microalgae,
996 *Mar Pollut Bull*, 57, 108–115, <https://doi.org/10.1016/j.marpolbul.2007.10.006>, 2008.

997

998 Yang, N., Lin, Y.-A., Merkel, C. A., DeMers, M. A., Qu, P.-P., Webb, E. A., Fu, F.-X., and
999 Hutchins, D. A.: Molecular mechanisms underlying iron and phosphorus co-limitation responses
1000 in the nitrogen-fixing cyanobacterium *Crocospaera*, *Isme J*, 16, 2702–2711,
1001 <https://doi.org/10.1038/s41396-022-01307-7>, 2022.

1002 Yoshida, M., Kuma, K., Iwade, S., Isoda, Y., Takata, H., and Yamada, M.: Effect of aging time
1003 on the availability of freshly precipitated ferric hydroxide to coastal marine diatoms, *Mar. Biol.*,
1004 149, 379–392, <https://doi.org/10.1007/s00227-005-0187-y>, 2006.

1005